

PAPER PRESENTED AT 26TH EU PVSEC, HAMBURG, GERMANY 2011

Solar cell generations over 40% efficiency

R. R. King*, D. Bhusari, D. Larrabee, X.-Q. Liu, E. Rehder, K. Edmondson, H. Cotal, R. K. Jones, J. H. Ermer, C. M. Fetzer, D. C. Law and N. H. Karam

Spectrolab, Inc., 12500 Gladstone Ave, Sylmar, CA 91342, USA

ABSTRACT

Multijunction III-V concentrator cells of several different types have demonstrated solar conversion efficiency over 40% since 2006, and represent the only third-generation photovoltaic technology to enter commercial power generation markets so far. The next stage of solar cell efficiency improvement, from 40% to 50%-efficient production cells, is perhaps the most important yet, since it is in this range that concentrator photovoltaic (CPV) systems can become the lowest cost option for solar electricity, competing with conventional power generation without government subsidies. The impact of 40% and 50% cell efficiency on cost-effective geographic regions for CPV systems is calculated in the continental US, Europe, and North Africa. We take a systematic look at a progression of multijunction cell architectures that will take us up to 50% efficiency, using modeling grounded in well-characterized solar cell materials systems of today's 40% cells, discussing the theoretical, materials science, and manufacturing considerations for the most promising approaches. The effects of varying solar spectrum and current balance on energy production in 4-junction, 5-junction, and 6-junction terrestrial concentrator cells are shown to be noticeable, but are far outweighed by the increased efficiency of these advanced cell designs. Production efficiency distributions of the last five generations of terrestrial concentrator solar cells are discussed. Experimental results are shown for a highly manufacturable, upright metamorphic 3-junction GaInP/GaInAs/Ge solar cell with 41.6% efficiency independently confirmed at 484 suns (48.4 W/cm^2) (AM1.5D, ASTM G173-03, 25 °C), the highest demonstrated for a cell of this type requiring a single metal-organic vapor-phase epitaxy growth run. Copyright © 2012 John Wiley & Sons, Ltd.

KEYWORDS

multijunction; high efficiency; concentrator; III-V; metamorphic; 4-junction, 5-junction, 6-junction; energy production; cost modeling

*Correspondence

Richard King, Spectrolab, Inc., 12500 Gladstone Ave, Sylmar, CA 91342, USA.

E-mail: rking@spectrolab.com

Received 2 September 2011; Revised 2 November 2011; Accepted 22 November 2011

1. INTRODUCTION

Multijunction III-V concentrator cells have the highest energy conversion efficiency of any solar cell technology, with several different types of cell architecture reaching over 40% efficiency since 2006 [1–7]. Such cells represent the only third-generation photovoltaic technology to enter commercial power generation markets so far, and continue to demonstrate what is possible for other emerging solar cell technologies that divide the sun's spectrum into discrete slices for higher efficiency, such as flat-plate multijunction polycrystalline semiconductor cells, tandem organic solar cells, and spectral splitting optical systems.

III-V multijunction concentrator cells using these high-efficiency innovations are now by far the dominant type of solar cells used in concentrator photovoltaic (CPV) solar electric systems, due to their dramatic efficiency advantages.

Photovoltaics have grown at a phenomenal rate of over 40% per year for the last decade, but much of this growth has been sustained by hefty government subsidies. To become a technology that truly changes the way the global community generates most of its electricity, photovoltaics will become too large to be helped substantially by funding from any government, and will need to be cost effective for bulk power generation without subsidies. Because of the III-V multijunction cell efficiency advances discussed previously and the corresponding reduction in collector area, concentrator photovoltaic systems promise dramatically lower costs, without government subsidies, than today's photovoltaic technologies.

The next stage of solar cell efficiency improvement, in the decade from 40% to 50%-efficient production cells, is perhaps the most important yet, because it is in this efficiency range that concentrator photovoltaic systems have the ability to generate solar electricity at rates well below

0.10 €/kWh \approx 0.14 \$/kWh over wide geographic areas. This allows CPV systems with 40%–50% cell efficiencies to compete effectively with conventional forms of power production, even without government subsidies.

Though multijunction cell efficiencies are still far from their theoretical efficiencies of over 70%, the effects of those physical limits can be felt in today's cells, and the rate of efficiency increase has begun to lessen. As 3-junction concentrator solar cell technology becomes more highly evolved, it has become increasingly evident that the next steps in efficiency will need to come from qualitatively new cell structures, rather than from iterative improvements of the existing 3-junction technology.

In this paper, we take a systematic look at the most promising multijunction cell architectures that will take us up to 50% efficiency, using empirically-based modeling grounded in well-characterized solar cell materials systems, discussing the theoretical, materials science, and manufacturing considerations for the most promising approaches.

2. GEOGRAPHIC AND ECONOMIC IMPACT OF HIGH EFFICIENCY

Sunlight is one of the most plentiful energy resources on earth. The amount of energy from the sun striking the planet is over 1.5×10^{22} J (15,000 EJ) each day, more than 10^4 times the 1.3 EJ daily energy consumption by human activity [8]. Clearly, solar energy is a sustainable resource, with energy input far exceeding the rate it is consumed. It is also, however, a dilute source of energy, requiring relatively large collector areas to generate solar electricity compared with, say, the lighting, appliances, vehicles, and manufacturing

processes that use it. The large areas required are at the heart of the cost of solar electricity. The large collector area must be encapsulated and supported by a certain amount of glass, metal, and plastic, to protect against the elements for many years and provide mechanical stability, whether the photovoltaic collector is a flat-plate panel or a CPV module. Although these are relatively inexpensive materials on a per-unit-weight basis, and module manufacturing methods are fairly straightforward, their cost places a lower limit on how inexpensive photovoltaic electricity can become for a given collector area, without even considering the cost of the particular photovoltaic cell technology used.

High efficiency is one of the few effective ways to reduce these fundamental module packaging and support costs of solar electricity. A 10%-efficient module technology requires 10 m^2 worth of materials and manufacturing for module packaging and support to generate 1 kW of electricity under 1000 W/m^2 incident intensity, whereas a 25%-efficient module requires 2.5 times less, or only 4 m^2 . As a result and somewhat counter-intuitively, more complicated and expensive PV cell technologies that also confer higher efficiency can frequently be less expensive at the module or full PV system level than modules based on lower efficiency cells.

The lower costs of PV systems with higher efficiency greatly expand the geographic regions in which they are cost-effective. Figure 1 is a map of the continental United States, with filled contours indicating the intensity of direct normal solar radiation, or direct normal irradiance, in units of kWh/(m² day) for each geographic location. Superimposed on this map are line contours indicating regions of cost effectiveness for three different cell efficiency and system optical efficiency cases. Here, cost

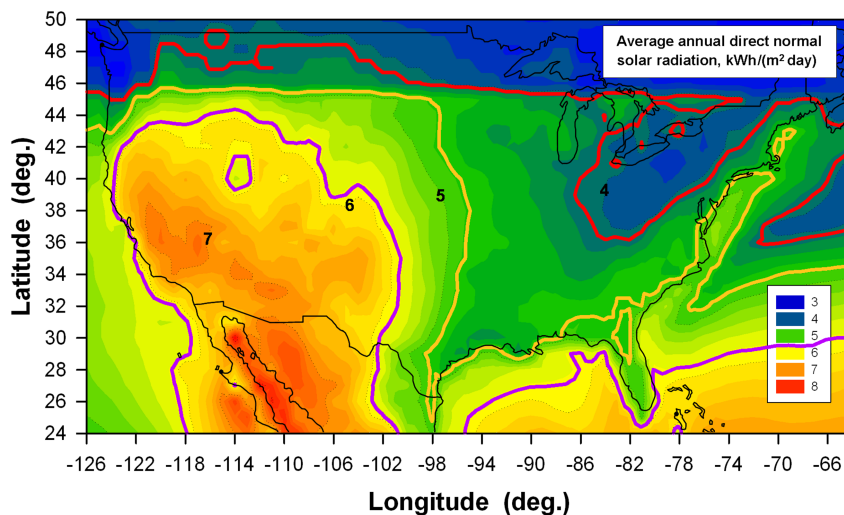


Figure 1. Map of the continental United States, with filled contours indicating annual average direct normal solar radiation, in units of kWh/(m² day), as well as colored line contours indicating regions of cost effectiveness (0.14 \$/kWh \approx 0.10 €/kWh of generated electricity) for three cases of concentrator photovoltaic (CPV) systems

- | | |
|-----------------|--|
| Case 1 (purple) | 40% cell and 80% optical eff., 50 W/cm^2 on cell \rightarrow 5.8 kWh/(m ² day) |
| Case 2 (orange) | 50% cell and 80% optical eff., 50 W/cm^2 on cell \rightarrow 4.8 kWh/(m ² day) |
| Case 3 (red) | 50% cell and 85% optical eff., 85 W/cm^2 on cell \rightarrow 4.1 kWh/(m ² day). |

effectiveness is taken to mean that solar electricity can be generated by a given concentrator photovoltaic technology for $0.14 \text{ \$/kWh} \approx 0.10 \text{ €/kWh}$, in 2011 currency, as an illustrative example. The cost per unit energy of conventional electricity generation is highly variable, depending on supply and demand in a given geographic and political region, but also on the structure of subsidies for conventional power generation, and the assumptions made about long-term costs of energy security, climate change, and other environmental effects for a given energy technology; no one energy cost value fits all markets. The value of $0.14 \text{ \$/kWh} \approx 0.10 \text{ €/kWh}$ provides a benchmark in this study, and the results may be scaled up or down for other values of present non-PV energy costs, as appropriate for different assumption sets and different energy markets.

Figure 2 is a similar figure showing direct normal solar radiation and cost-effectiveness contours for the European continent and North Africa. For both Figures 1 and 2, the direct normal irradiance at each latitude and longitude point is from the National Aeronautics and Space Administration Atmospheric Science Data Center Surface meteorology and Solar Energy (SSE) database [9], which provides solar resource data for the entire globe, and which shows similar geographic trends in the continental United States as National Renewable Energy Laboratory solar resource databases, such as [10].

Three different sets of CPV cell and system efficiency are represented in Figures 1 and 2 by the colored, bold line contours:

- (i) 40% CPV cell efficiency measured under standard test conditions (STC), 80% system optical efficiency, and 50.0 W/cm^2 (500 suns) incident on the cells;
- (ii) 50% cell efficiency under STC, 80% system optical efficiency, and 50 W/cm^2 on the cells; and
- (iii) 50% cell efficiency under STC, 85% system optical efficiency, and 85 W/cm^2 (850 suns) incident on the cells.

In Figure 1, one can see that the range of cost effectiveness with today's 40%-efficient CPV cells is broadened from the desert southwest US in Case 1, to a much larger portion of the American midwest, Florida, and parts of the southeastern US for Case 2 which is the same in all respects except for the increase of cell efficiency to 50% at STC, for the cost parameters used in this study. For the European continent in Figure 2, the transition from 40% to 50%-efficient CPV cells at STC causes the cost effective region to encompass most of the Iberian Peninsula, Turkey, and coastal regions throughout Europe.

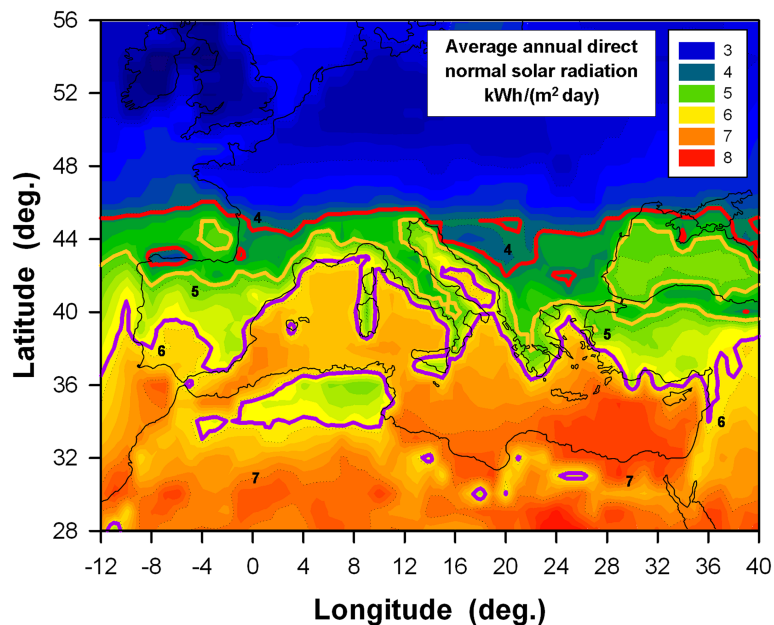


Figure 2. Map of the European continent and North Africa, with filled contours indicating annual average direct normal solar radiation, in units of $\text{kWh}/(\text{m}^2 \text{ day})$, as well as colored line contours indicating regions of cost effectiveness ($0.14 \text{ \$/kWh} \approx 0.10 \text{ €/kWh}$ of generated electricity) for three cases of concentrator photovoltaic (CPV) systems

Case 1 (purple)	40% cell and 80% optical eff., 50 W/cm^2 on cell $\rightarrow 5.8 \text{ kWh}/(\text{m}^2 \text{ day})$
Case 2 (orange)	50% cell and 80% optical eff., 50 W/cm^2 on cell $\rightarrow 4.8 \text{ kWh}/(\text{m}^2 \text{ day})$
Case 3 (red)	50% cell and 85% optical eff., 85 W/cm^2 on cell $\rightarrow 4.1 \text{ kWh}/(\text{m}^2 \text{ day})$.

If the increase in cell efficiency to 50% can be coupled with ambitious improvements in CPV system optical efficiency as in Case 3, most of the contiguous 48 states of the US are in the cost effective region for CPV deployment as shown in Figure 1, including the southeastern US and eastern US seaboard, without government subsidies. In Europe, the region of cost effectiveness for CPV systems expands to include southern France, and all of Italy and Greece, as plotted in Figure 2.

The cost accounting for CPV systems is straightforward in principle. In a simplified approach, the system cost per unit of generated energy, $(C/E)_{\text{system}}$, is the system cost per unit module aperture area, divided by the energy per area generated over a given payback time

$$\left(\frac{C}{E}\right)_{\text{system}} = \frac{C_{\text{mod}} + C_{\text{BOS}} + C_{\text{pwr cond}}}{A_{\text{mod}} \text{Int}_{\text{annual avg}} \eta_{\text{AC,system}} T_{\text{payback}}} \quad (1)$$

where

C_{mod}	cost of module (cells, cell packaging, and module packaging)
C_{BOS}	cost of balance-of-system (BOS) (e.g., support structures, wiring, installation, operations and maintenance, financing), excluding power conditioning
$C_{\text{pwr cond}}$	cost of power conditioning unit (inverter) for system
A_{mod}	aperture area of modules in system
$\text{Int}_{\text{annual avg}}$	annual average intensity of solar resource (direct normal for concentrator, global for flat-plate) in a given geographic location, in units of kWh/(m ² day)
$\eta_{\text{AC,system}}$	total efficiency of PV system, from sunlight to AC power
T_{payback}	time allotted to payback capital cost of system, from power generated.

The cost effectiveness contours in Figures 1 and 2 were found by noting that for a given cost per unit generated energy $(C/E)_{\text{system}}$, taken to be 0.14 \$/kWh \approx 0.10 €/kWh in this study, the annual average intensity of sunlight $\text{Int}_{\text{annual avg}}$ that can support this cost is

$$\text{Int}_{\text{annual avg}} = \frac{C_{\text{mod}} + C_{\text{BOS}} + C_{\text{pwr cond}}}{A_{\text{mod}} \left(\frac{C}{E}\right)_{\text{system}} \eta_{\text{AC,system}} T_{\text{payback}}} \quad (2)$$

The greatest uncertainty in this analysis is in the cost of the non-cell components of the CPV module, and in the CPV system BOS costs. To provide a systematic estimate of these costs, US Department of Energy (DOE) current ‘‘Business as Usual’’ 2016 cost projections for utility scale PV systems were used [11], for module, BOS, and power electronics costs in all three cases. Using estimated III-V multijunction CPV cell costs of 7.50 \$/cm² of cell aperture area plus 2.50 \$/cm² cell packaging costs, for a round number of 10 \$/cm² for CPV cells plus cell packaging, the non-cell module costs can be extracted from the total module cost and are 122 \$/m² for all three cases as described in more

detail in Appendix A. The DOE balance of system costs without tracking are 260 \$/m², to which the extra costs of the tracking mechanism for CPV systems are added. The resulting total CPV system cost per unit module aperture area $(C_{\text{system}}/A_{\text{mod}})$ calculated in this way is 597 to 654 \$/m². As a check, this is well within the range between high and low-cost estimates in [12].

The efficiency of the overall CPV system starts with the cell efficiency at STC, but also includes: the CPV system optical efficiency; power conditioning efficiency; fraction of power at STC remaining at operating temperature; fraction of power remaining because of the difference between the standard design solar spectrum and average actual spectrum; fraction of energy production remaining because of changes in the actual spectrum over the day and year with respect to the average actual spectrum; and fraction of energy production remaining because of tracking errors, as detailed in Appendix B. Total system efficiencies are 26.8%, 33.5%, and 35.6% for Cases 1, 2, and 3, respectively. The payback period T_{payback} is chosen to be 8 years.

With these cost and efficiency parameters, the threshold direct normal solar radiation level for cost effective CPV energy production at 0.14 \$/kWh \approx 0.10 €/kWh are the following:

- a total of 5.8 kWh/(m² day) for Case 1 (40% cell and 80% optical efficiency, 50 W/cm² on cell);
- a total of 4.8 kWh/(m² day) for Case 2 (50% cell and 80% optical efficiency, 50 W/cm² on cell); and
- a total of 4.1 kWh/(m² day) for Case 3 (50% cell and 85% optical efficiency, 85 W/cm² on cell),

as shown in the contours in Figures 1 and 2. For comparison, using the same cost parameters for a Case 4 using silicon CPV cells with 26% efficiency under STC at 50.0 W/cm², with 2.50 \$/cm² cell packaging cost as before, but optimistically assuming zero cost for the Si cells, leads to a total CPV system efficiency of 16.5% for Case 4, confining the region of cost effectiveness to the limited areas with direct normal solar radiation greater than 7.5 kWh/(m² day).

Because of the uncertainty in cost inputs, these cost projections are meant to be only illustrative; actual energy costs may be higher—or lower—depending on specifics of the CPV system. The trends are clear, however, the high efficiency of 40% III-V multijunction CPV cells, and ultimately increasing efficiency to 50% are vitally important for reducing the area of non-cell module components and support structures, as well as the required area of CPV cells themselves, thereby expanding the range of cost effectiveness of photovoltaics. It is significant that large geographic regions can support economically viable solar electricity generation, even with the ‘‘Business as Usual’’ cost parameters used here. With further reductions in the cost of module, BOS, and power electronics components, CPV systems could push into even higher latitudes with lower direct normal irradiance and still remain cost effective.

3. HIGH-EFFICIENCY MULTIJUNCTION CELL STRUCTURES

Solar cell efficiencies can be dramatically improved by dividing the broad solar spectrum up into smaller wavelength ranges, each of which can be converted more efficiently, through the use of multijunction cells. Multijunction CPV solar cells are the only third-generation photovoltaic technology—cells with double or triple the 15%–20% efficiencies targeted by first and second generation PV cells [13] and able to overcome the Shockley–Queisser efficiency limit for single-junction cells—that are now in commercial production. A large measure of success has been achieved with 3-junction GaInP/GaInAs/Ge concentrator solar cells operating on this principle, the first solar cell technology of any type to reach over 40% efficiency [1], and which is now the baseline technology for 40% production CPV cells [14]. As efficient as they are, however, this baseline 3-junction design is still far from the optimum combination of subcell bandgaps, and far from its efficiency potential.

Ideal efficiencies of over 59% are possible for 4-junction cells, and for 5-junction and 6-junction terrestrial concentrator cells, efficiencies over 60% are achievable in principle [15,16]. By providing a higher theoretical efficiency, solar cell architectures with 4-junction, 5-junction, and 6-junction offer a route to greater average efficiencies in high-volume manufacturing as well. Significantly, energy production modeling for 4-junction, 5-junction, and 6-junction CPV cells with the changing terrestrial spectrum that occurs with changing sun angle over the course of the day indicates that such cells have much greater energy production than 3-junction cells, retaining

most of their advantage in efficiency at the design point for production of kilowatt hours in the field [16].

Because the efficiency range from 40% to 50% is so leveraging, spanning a tipping point for which vast geographic regions become available for economic CPV plant operation without government subsidies, it is important to examine the variety of multijunction cell configurations that can take us well beyond 40%, even though these structures are generally more complex and technologically challenging than today’s 3-junction cells. A progression of sample high-efficiency concentrator solar cell structures is shown in Figure 3, beginning with 3-junction cells of today and the near future, and advancing through 4-junction, 5-junction, and 6-junction cells with a variety of technologies. These include upright metamorphic (MM) cells, inverted metamorphic (IMM) cells with single, double, and triple (MMX3) graded buffer layers, epitaxial Ge and SiGe subcells, semiconductor bonding technology, and dilute nitride GaInNAsSb subcells.

Projected average efficiencies in production are shown beneath each example cell type in Figure 3. The efficiencies are calculated using cell parameters—such as the series resistance, subcell bandgap-voltage offsets, diode ideality factors, reflectance, grid shadowing, and other non-ideal current losses—that are consistent with the nominal 40% production average efficiency of Spectrolab C4MJ cells, shown second from the left in Figure 3(b). So, provided that the new semiconductor materials involved can reach the required material quality, the calculated efficiencies in Figure 3 are the potential average efficiencies in manufacturing based on the various multijunction cell bandgap combinations; champion cell efficiencies can be still higher.

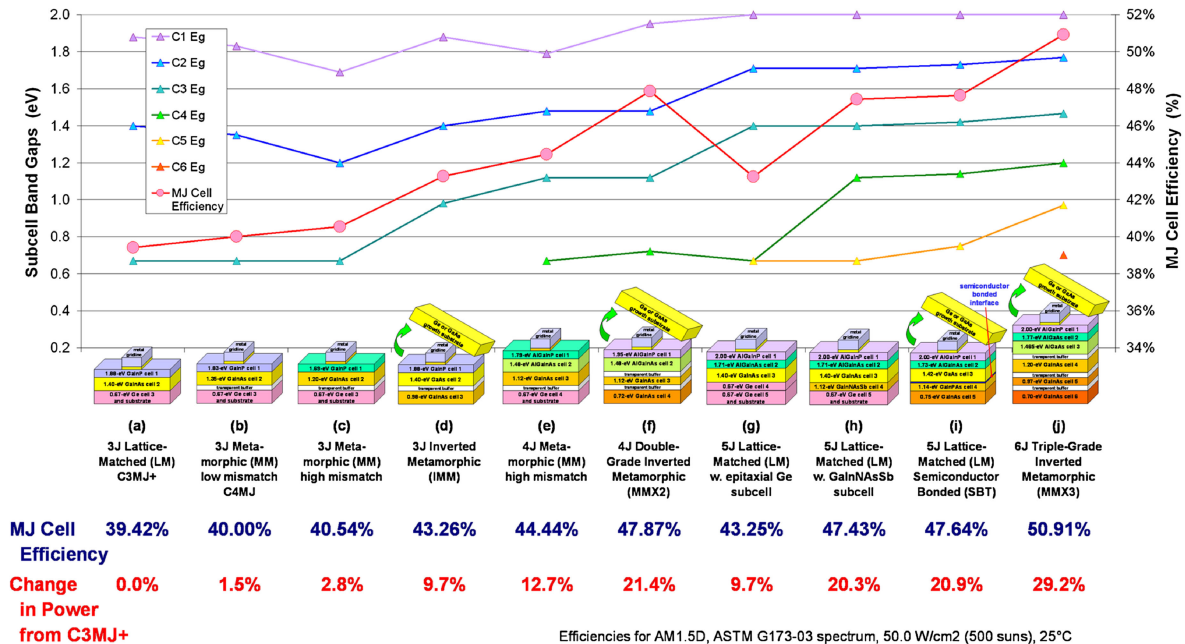


Figure 3. Progression of various terrestrial concentrator solar cell designs, beginning with today’s 3-junction C3MJ+ and 40% C4MJ cells, and increasing efficiency to over 50% under the concentrated AM1.5D spectrum.

The cell designs in Figure 3 represent only a few of the possible cell architectures leading to efficiencies from 40% to 50% but each serves as an example of the design considerations, some positive, some negative, that must be contended with on this path. Beginning toward the left, Figure 3(b) shows a 3-junction upright MM cell structure. A larger schematic cross-section of this cell design, which corresponds to the 40% production average efficiency C4MJ cell, is shown in Figure 4(a). Calculated light *I*-*V* curves for each subcell and the integrated 3 J cell are plotted in Figure 4(b). Such 3-junction upright metamorphic GaInP/GaInAs/Ge concentrator cells [1,3,4,17] have higher efficiency in principle than their lattice-matched (LM) counterparts, because the larger lattice constant in the metamorphic upper subcells (subcells 1 and 2) allows their bandgap to be lowered. For the wavelength distribution of the solar spectrum, the tradeoff between current and voltage is favorable for the lower bandgaps of the metamorphic upper subcells. This tradeoff results in maximum efficiency for an MM GaInAs subcell 2 composition of around 16%–17% indium in 3-junction GaInP/GaInAs/Ge cells [1,17,18], and with the composition of the MM GaInP subcell 1 at the same lattice constant. Figure 3(c) shows a schematic cross-section of this cell type, with 40.5% projected production average efficiency under the AM1.5D solar spectrum. The lower lattice mismatch and subcell 2 composition of 5%-In GaInAs in

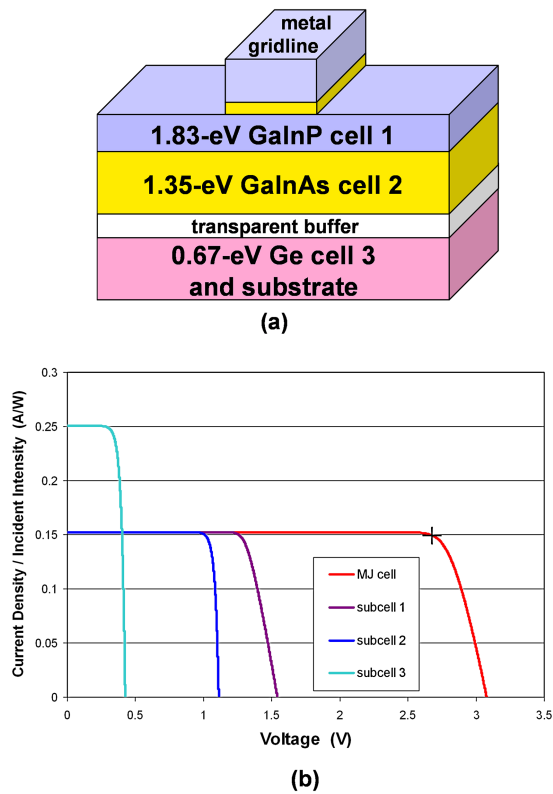


Figure 4. (a) Cross-sectional diagram and (b) illuminated *I*-*V* curves for subcells and the full multijunction cell for a 3-junction, upright metamorphic (MM) GaInP/GaInAs/Ge concentrator solar cell (C4MJ), with modeled production average efficiency of 40.0% at 500 suns (50.0 W/cm²).

40%-efficient C4MJ cells represent a more robust, lower manufacturing cost approach than cells with higher indium content and lattice mismatch in the upper subcells, that still delivers substantial gain in cell efficiency, as well as providing the first step for commercial solar cells on the technology path to metamorphic cell architectures.

Continuing in the family of upright metamorphic cells, 4-junction AlGaInP/AlGaInAs/GaInAs/Ge upright metamorphic cells as shown in Figure 3(e) and Figure 5 are attractive candidates for the next generation of concentrator solar cells, because they have a projected average efficiency over 44%, well in excess of the nominal 40% production efficiency of present C4MJ cells; they require only a single growth run and a single metamorphic buffer; they utilize upright layer growth, avoiding thermal budget and dopant memory issues that can occur in inverted growth; and avoid the extra process complexity, cost, and yield loss associated with handle bonding and substrate removal for inverted metamorphic cells. However, questions remain about whether the highly lattice-mismatched AlGaInP and AlGaInAs subcells, at around 1.5% mismatch to the lattice constant of the Ge growth substrate, corresponding to

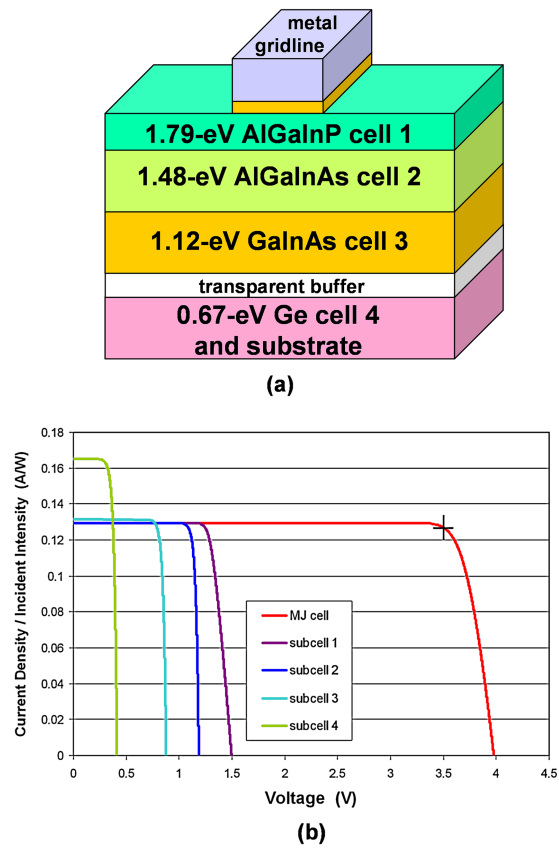


Figure 5. (a) Cross-sectional diagram and (b) illuminated *I*-*V* curves for subcells and the full multijunction cell for a 4-junction, upright metamorphic (MM) AlGaInP/AlGaInAs/GaInAs/Ge concentrator solar cell, with modeled production average efficiency of 44.4% at 500 suns (50.0 W/cm²).

22%-In GaInAs, and with substantial Al content, can have the required minority-carrier lifetimes and mobilities.

In another example, 5-junction cells with a dual-junction Ge/Ge subcell combination for the lower two subcells [19], using an epitaxially-grown Ge subcell 4, with an AlGaInP/AlGaInAs/GaInAs/Ge/Ge LM 5-junction structure as shown in Figure 3(g) and Figure 6, also has an attractive projected 43.2% average efficiency. Other metamorphic variations using an epitaxial SiGe or SiGeSn subcell with higher bandgap than Ge can have still higher efficiency. The cell shown in Figure 6 is fully lattice-matched, simplifying manufacturing and avoiding the time and materials associated with growth of a metamorphic buffer. The upright structure of the 5-junction Ge/Ge cell also has the significant reduced thermal budget, reduced dopant memory, and reduced processing cost advantages described in the last paragraph, compared with inverted metamorphic structures. However, questions remain about the material quality, minority-carrier properties, and high degree of transparency needed for the epitaxial Ge, SiGe, or SiGeSn subcells.

The need for a semiconductor with ~1-eV bandgap at or near the lattice constant of Ge or GaAs can be satisfied in principle using dilute nitride semiconductors such as GaInNAS

or GaInNASb, with compositions around just 0.5% to 3% nitrogen [20–27]. GaInNAS subcells grown by molecular beam epitaxy have demonstrated the necessary level of current density to be current matched in a 3-junction GaInP/GaAs/GaInNAS or 4-junction GaInP/GaAs/GaInNAS/Ge solar cell [28]. Recently, a 3-junction cell using a dilute nitride bottom subcell was independently measured to have a record efficiency of 43.5% [7]. Doping control and long minority-carrier diffusion lengths have historically been challenging to achieve in GaInNAS subcells grown by low cost, high throughput metal-organic vapor-phase epitaxy (MOVPE), though rich opportunities exist for growing these highly versatile ~1-eV GaInNAS(Sb) materials by low-cost growth methods.

Given the challenges in achieving high current densities in dilute nitride GaInNAS(Sb) materials, it can be advantageous to divide the solar spectrum more finely with the multijunction cell structure, such as a 5-junction or 6-junction cell, resulting in a high-voltage, lower-current multijunction cell for which the GaInNAS(Sb) cell can be current matched [19]. MOVPE GaInNAS cells were monolithically integrated into the first 6-junction cells in 2004 [29], and improved external quantum efficiencies were demonstrated in [30]. GaInNAS cells with 1.168-eV bandgap have been grown at Spectrolab on 100-mm-diameter Ge wafers, in production-scale MOVPE reactors capable of growing 12 wafers per run at rates of 15–30 μm per hour, with open-circuit voltage V_{oc} of 684 mV at 1 sun. This bandgap-voltage offset $(E_g/q) - V_{oc}$ of 484 mV can be improved upon with further work and can already support many of the high-efficiency multijunction cell architectures envisioned with dilute nitride subcells. A 5-junction AlGaInP/AlGaInAs/GaInAs/GaInNAS(Sb)/Ge upright LM cell structure and projected average efficiency are shown in Figure 3(h) and Figure 7, with a projected production average efficiency of 47.4%. Again, the upright, LM structure of this design carries the formidable advantages of reduced thermal budget and dopant memory issues, and avoidance of the extra process complexity, cost, and yield loss associated with handle bonding and substrate removal, compared with inverted metamorphic cells. Integrated 4-junction cells with a similar subcell bandgap combination as the 5-junction cell, but with the dilute nitride subcell 4 absent, have been built and have reached measured efficiencies of 36.9% at 500 suns (50.0 W/cm^2) with relatively little optimization to date [31].

In spite of the greater expense and complexity associated with handle bonding and substrate removal for IMM cell structures, their ability to combine high bandgap, LM cells with low bandgap, metamorphic cells, with a high degree of bandgap flexibility, allows for very high efficiencies in practice. An example of a 6-junction AlGaInP/AlGaAs/AlGaAs/GaInAs/GaInAs/GaInAs IMM cell with an MMX3 buffer structure is shown in Figure 3(j) and Figure 8. The inverted metamorphic structure allows the bandgap combination needed for a projected 50.9% production average efficiency to be grown in a single growth run, albeit one with three metamorphic buffers. Questions about the achievable electronic properties of these new solar cell compositions and structures need to be answered experimentally,

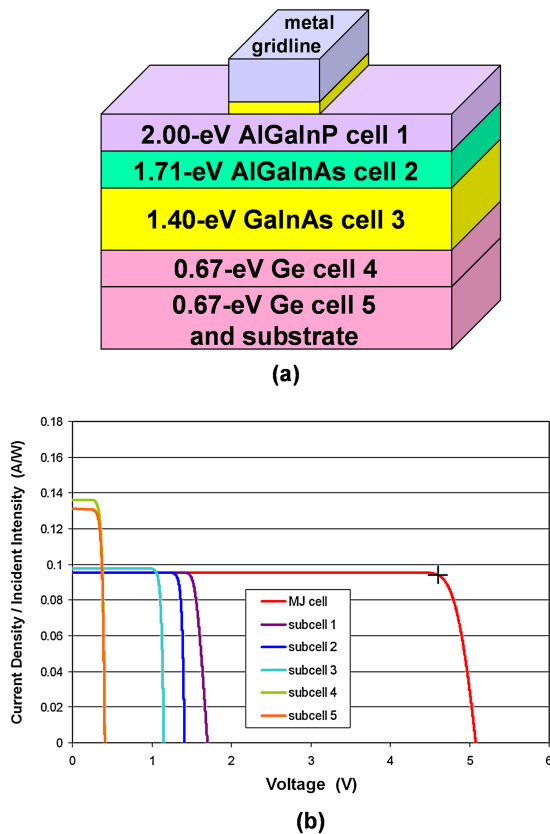


Figure 6. (a) Cross-sectional diagram and (b) illuminated I - V curves for subcells and the full multijunction cell for a 5-junction, lattice-matched AlGaInP/AlGaInAs/GaInAs/epitaxial Ge/Ge concentrator solar cell, with modeled production average efficiency of 43.2% at 500 suns (50.0 W/cm^2).

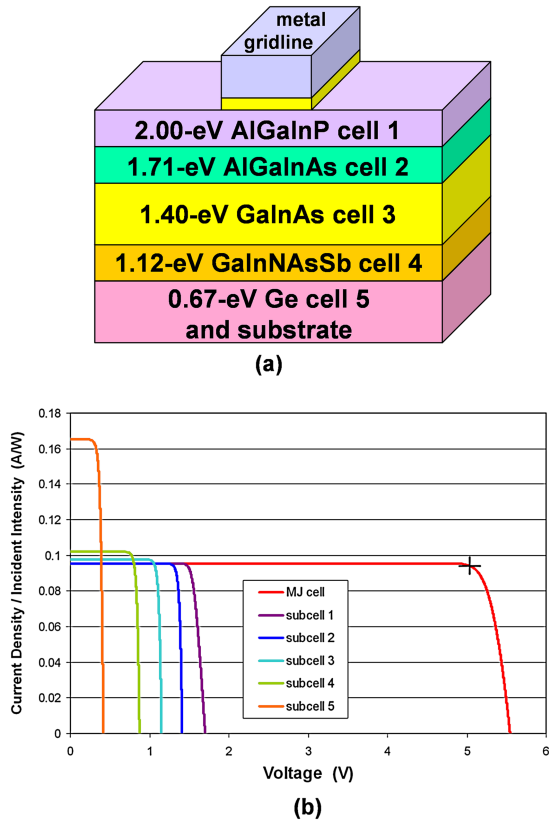


Figure 7. (a) Cross-sectional diagram and (b) illuminated I - V curves for subcells and the full multijunction cell for a 5-junction, lattice-matched AlGaInP/AlGaInAs/GaInAs/dilute nitride GaInNAS(Sb)/Ge concentrator solar cell, with modeled production average efficiency of 47.4% at 500 suns (50.0 W/cm^2).

and these empirical studies will show which of the many promising theoretical solar cell designs are best suited to high-volume production.

4. ENERGY PRODUCTION

As for all solar cells, energy production over the course of the day and year is of great interest, in addition to the efficiency under standard conditions [16,32–3]. These two figures of merit are naturally very strongly correlated, but it is energy production that directly impacts the revenue, and therefore the cost-effectiveness, of a photovoltaic system.

The energy production of 4-junction, 5-junction, and 6-junction cells was modeled in detail in [16], showing that the effects of varying current balance in 4-junction, 5-junction, and 6-junction terrestrial concentrator cells with changes in incident spectrum are noticeable, but are far outweighed by the increased efficiency of these advanced cell designs. The similarity in the 4-junction and 5-junction efficiencies in Figure 9 is due to the specific subcell bandgaps chose for these cases, as given in [16]; for other bandgap choices, 5-junction cells may show a larger efficiency advantage over 4-junction cells. Figure 9(a) below from [16] shows that by 7.50 h

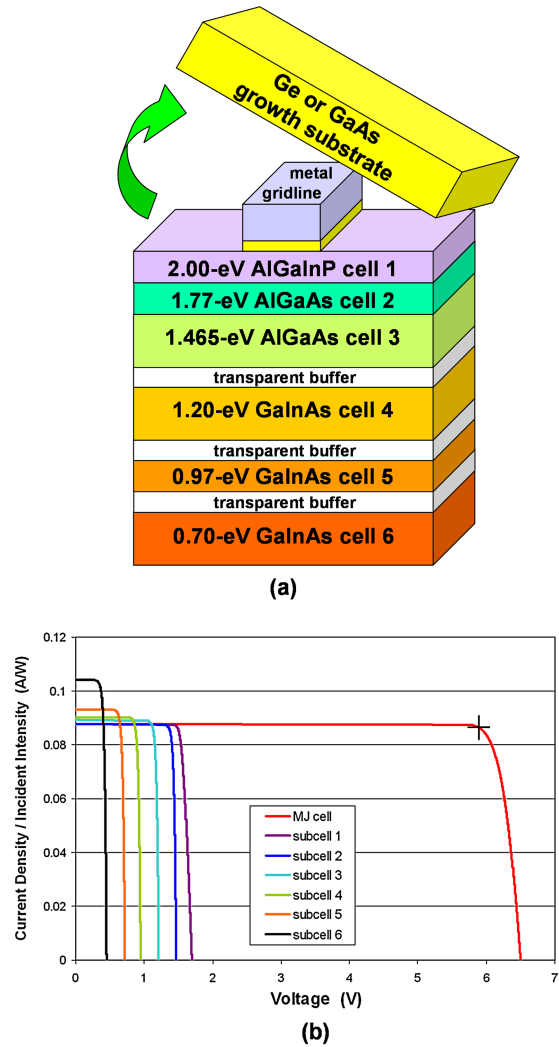


Figure 8. (a) Cross-sectional diagram and (b) illuminated I - V curves for subcells and the full multijunction cell for a 6-junction, inverted metamorphic (IMM) cell and three transparent graded buffer regions (MMX3), with an AlGaInP/AlGaAs/AlGaAs/GaInAs/GaInAs/GaInAs structure, and with modeled production average efficiency of 50.9% at 500 suns (50.0 W/cm^2).

(7:30 AM) on a representative day (the autumnal equinox), the 6-junction cell efficiency exceeds that of the 3-junction, 4-junction, and 5-junction cells, and thereafter is the highest efficiency cell type over the most significant energy-producing hours of the day. The 6-junction cell has higher total energy production over this typical day than designs with fewer subcells, as shown in Figure 9(b), including conventional LM 3-junction cells, owing to the higher efficiency design, lower carrier thermalization losses, and lower series resistance losses of the 6-junction cell. Table I from [16] shows that the effect of changing solar spectrum over the course of the day lowers energy production by only ~1.1% relative in going from 3-junction to 6-junction cells, whereas the efficiency of 6-junction cells under STC is over 23% higher on a relative basis (>23% higher power) than the 3-junction cells

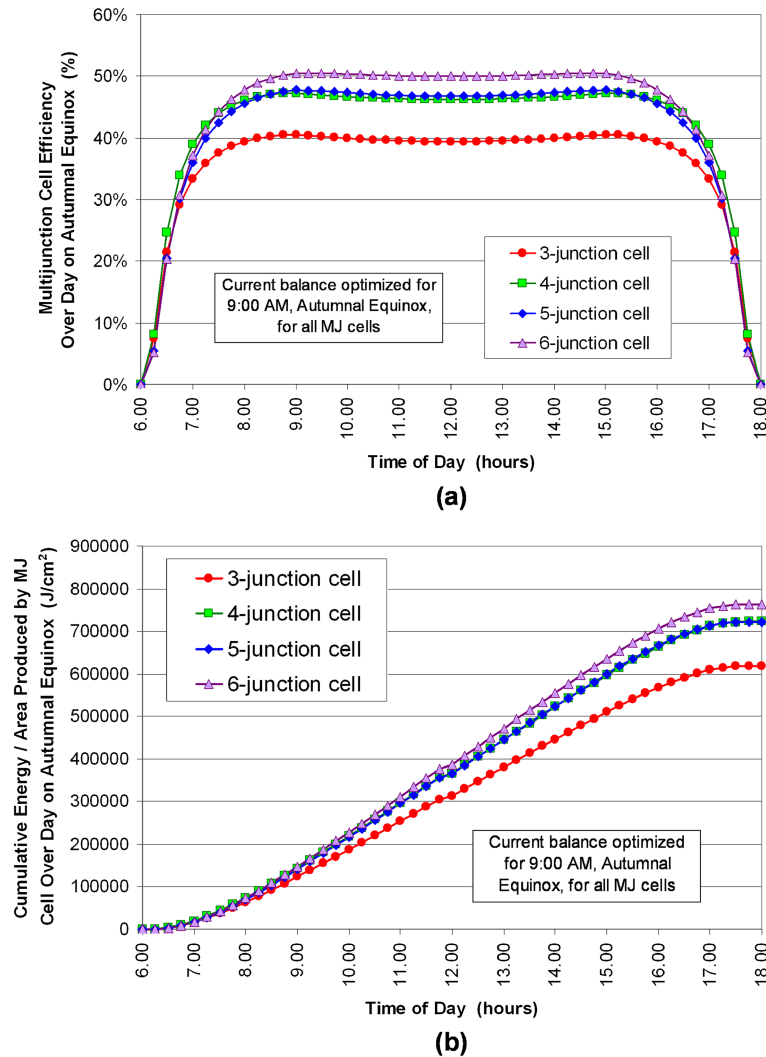


Figure 9. (a) Multijunction cell efficiency over the course of the day, modeled for 3-junction, 4-junction, 5-junction, and 6-junction cells on the autumnal equinox and (b) modeled cumulative energy produced per unit area over the day, clearly showing that the higher efficiency 4-junction and 5-junction cell designs produce more energy than conventional 3-junction cells, and 6-junction cells produce more than any of the other cell designs by the end of the day (from [16]).

in Table I. Thus, having greater than three junctions is not an overall impediment to the energy production of a multijunction cell, and because a greater number of junctions also allow for higher efficiency, such cells with 4-junction, 5-junction, and 6-junction are actually a route toward higher energy production that is difficult to avoid.

5. EXPERIMENTAL RESULTS

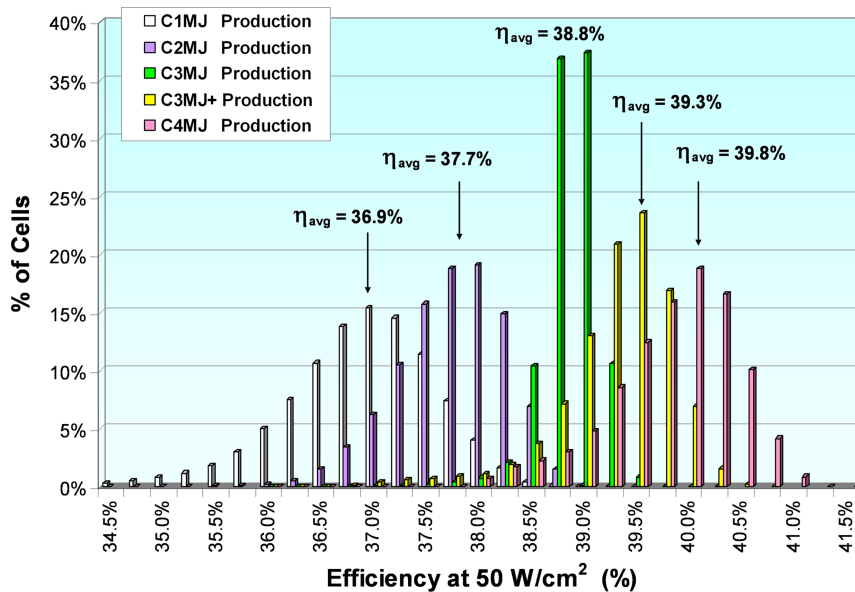
Experimental results are given in this section for some of today's state-of-the-art multijunction cells. Figure 10 charts efficiency distributions for the last five generations of Spectrolab production terrestrial concentrator cells at 500 suns (50.0 W/cm²): the C1MJ, C2MJ, C3MJ, C3MJ+, and C4MJ cells. Upright metamorphic 3-junction GaInP/GaInAs/Ge concentrator cells, of the type that were first to reach over the 40%

efficiency milestone, have now entered manufacturing production as the C4MJ cell. As shown in Figure 10, manufacturing production of the C4MJ terrestrial concentrator cell has demonstrated an average efficiency of 39.8% to date and is expected climb to the nominal 40% average efficiency for C4MJ as production continues.

Measurements are shown here for the first time of an upright metamorphic 3-junction GaInP/GaInAs/Ge solar cell with independently-confirmed 41.6% efficiency at 484 suns (48.4 W/cm²) (AM1.5D, ASTM G173-03, 25 °C), the highest yet demonstrated for an upright metamorphic solar cell of this highly manufacturable type, requiring a single MOVPE growth run. This metamorphic cell result matches the earlier record efficiency of 41.6% on a LM 3-junction GaInP/GaInAs/Ge cell [5]. The present metamorphic cell result is particularly remarkable because it was achieved at the

Table I. Comparison of key energy production parameters of: Peak multijunction solar cell efficiency during the day; Efficiency over the day; and Spectrum utilization efficiency over the day as defined in the table, calculated for 3, 4, 5, and 6-junction cells, from [16].

	3-junction	4-junction	5-junction	6-junction
Peak multijunction solar cell efficiency during day	40.5%	47.2%	47.7%	50.5%
Efficiency over day = Cell output energy during day/ Energy in incident spectrum during day	38.6%	45.1%	45.1%	47.7%
Spectrum utilization factor over day = Efficiency over day/ Peak multijunction solar cell efficiency	0.954	0.956	0.944	0.943

**Figure 10.** Efficiency histograms of the last five generations of Spectrolab terrestrial concentrator cell products, from the C1MJ cell with 36.9% average production efficiency, C2MJ with 37.7%, C3MJ with 38.8%, C3MJ+ with 39.3%, and production data for the newly introduced upright metamorphic C4MJ solar cell at 39.8% to date. Average efficiency for the C4MJ cell is anticipated to reach 40% with continued refinement of production processes.

relatively high concentration of 484 suns (48.4 W/cm^2), and on a fairly large concentrator cell with 1.0 cm^2 aperture area. The measured light I - V curve for this cell is shown in Figure 11(a), and the dependence of measured efficiency as a function of incident intensity is plotted in Figure 11(b). The efficiency of this metamorphic 3-junction cell is still over 41% for incident intensities above 740 suns (74.0 W/cm^2).

6. SUMMARY

The current path from 40% to 50% terrestrial concentrator cell efficiency is shown to markedly widen the geographic areas for which solar electricity can be generated cost effectively in the US and Europe. A progression of future multijunction cell structures is shown and modeled, with efficiencies ranging from the present-day C3MJ+ and 40% C4MJ 3-junction cells,

to cell designs with over 50% projected average efficiency. The efficiency advantage of cell architectures with 4, 5, and 6 junctions—as many cell designs on the path to 50% efficiency are—far outweighs the current balance effects of variable spectrum over the course of a typical day, giving such cells greater energy production than for conventional 3-junction cells. Efficiency distributions for the type of upright metamorphic 3-junction concentrator cell that first exceeded the 40% efficiency milestone, now in production as the C4MJ cell, average 39.8% at 500 suns (50.0 W/cm^2). Independently confirmed light I - V measurements are given for a metamorphic 3-junction GaInP/GaInAs/Ge solar cell of 41.6% at 484 suns (48.4 W/cm^2), the highest efficiency yet demonstrated for this type of cell using a single MOVPE growth run. If minority-carrier properties comparable with those in today's 3-junction cells can be maintained, the new solar cell materials and structures described here ranging up to 50% projected average efficiency promise to open wide

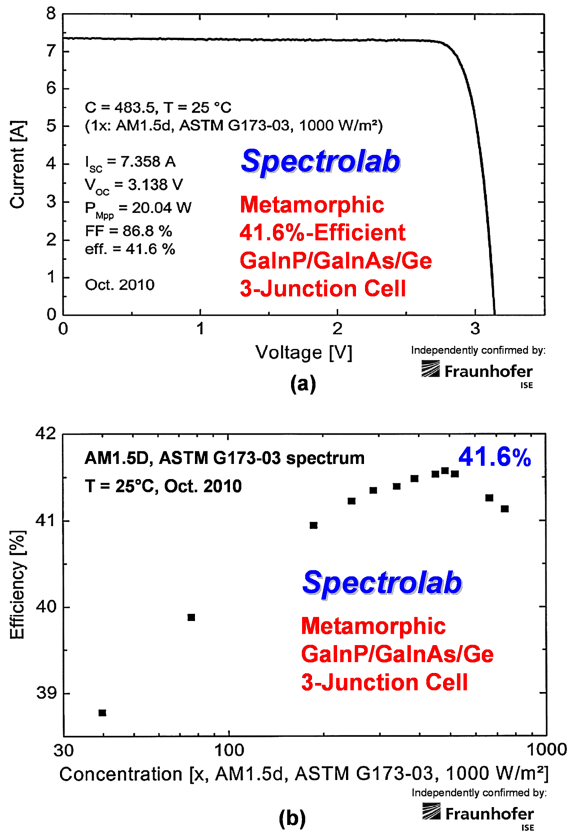


Figure 11. (a) Light I - V characteristic of a metamorphic 3-junction Spectrolab cell with 41.6% efficiency at 484 suns (48.4 W/cm^2), the highest yet achieved for a solar cell using a single MOVPE growth run; and (b) measured efficiency as a function of incident intensity, or concentration, for the 41.6%-efficient metamorphic 3-junction Spectrolab cell. The results were independently confirmed by the Fraunhofer Institute for Solar Energy (ISE) solar cell calibration lab.

geographic regions in the United States, Europe, and North Africa, for cost-effective concentrator photovoltaic power.

ACKNOWLEDGEMENTS

The authors would like to thank Daryl Myers at NREL for help with the wide array of solar resource databases available, Gerald Siefer and the photovoltaic calibration laboratory (CalLab) at Fraunhofer Institute for Solar Energy (ISE) for calibrated solar cell measurements, Omar Al-Taher, Pete Hebert, Randy Brandt, Peichen Pien, Shoghig Mesropian, Dimitri Krut, Kent Barbour, Mark Takahashi, Andrey Masalykin, John Frost, and the entire multijunction solar cell team at Spectrolab.

REFERENCES

1. King RR, Law DC, Edmondson KM, Fetzer CM, Kinsey GS, Yoon H, Sherif RA, Karam NH. 40%

efficient metamorphic GaInP/GaInAs/Ge multijunction solar cells. *Applied Physics Letters* 2007; **90**: 183516, doi: 10.1063/1.2734507.

2. Geisz JF, Friedman DJ, Ward JS, Duda A, Olavarria WJ, Moriarty TE, Kiehl JT, Romero MJ, Norman AG, Jones KM. 40.8% efficient inverted triple-junction solar cell with two independently metamorphic junctions. *Applied Physics Letters* 2008; **93**: 123505, doi:10.1063/1.2988497.
3. Dimroth F, Guter W, Schone J, Welser E, Steiner M, Oliva E, Wekkeli A, Siefer G, Philipps SP, Bett AW. Metamorphic GaInP/GaInAs/Ge triple-junction solar cells with > 41% efficiency. *34th IEEE Photovoltaic Specialists Conf. (PVSC), Philadelphia, PA 2009*; 1038, doi: 10.1109/PVSC.2009.5411199.
4. Guter W, Schone J, Philipps SP, Steiner M, Siefer G, Wekkeli A, Welser E, Oliva E, Bett AW, Dimroth F. Current-matched triple-junction solar cell reaching 41.1% conversion efficiency under concentrated sunlight. *Applied Physics Letters* 2009; **94**: 223504, doi: 10.1063/1.3148341.
5. King RR, Boca A, Hong W, Liu X-Q, Bhusari D, Larrabee D, Edmondson KM, Law DC, Fetzer CM, Mesropian S, Karam NH. Band-Gap-Engineered Architectures for High-Efficiency Multijunction Concentrator Solar Cells. *24th European Photovoltaic Solar Energy Conference (EU PVSEC), Hamburg, Germany 2009*; 55, ISBN 3-936338-25-6.
6. Wojtczuk S, Chiu P, Zhang X, Derkacs D, Harris C, Pulver D, Timmons M. InGaP/GaAs/InGaAs Concentrators Using Bi-Facial Epigrowth. *35th IEEE Photovoltaic Specialists Conf. (PVSC), Honolulu, HI 2010*.
7. Solar Junction press release, April 14, 2011, Diandra Weldon, http://www.sjsolar.com/downloads/Solar_Junction_World_Record_%20Efficiency_14April11.pdf.
8. U.S. Energy Information Administration, International Energy Annual 2004, released May-July 2006, <http://www.eia.doe.gov/iea/overview.html>.
9. National Aeronautics and Space Administration (NASA) Atmospheric Science Data Center, Surface meteorology and Solar Energy (SSE), Release 6.0, Meteorology and Solar Energy, Regional data subsets, <http://eosweb.larc.nasa.gov/cgi-bin/sse/sse.cgi?s01#s01>.
10. National Renewable Energy Laboratory (NREL), Dynamic Maps, GIS Data, & Analysis Tools, Concentrating Solar Power Radiation (10 km)—Static Maps, Annual, February 2009, http://www.nrel.gov/gis/images/map_csp_us_10km_annual_feb2009.jpg.
11. U.S. Dept. of Energy, Energy Efficiency and Renewable Energy (EERE), Funding Opportunity Exchange, DE-FOA-0000492: Foundational Program to Advance Cell Efficiency (F-PACE), FULL TEXT, PDF: Amendment 002 - Foundational Program to Advance Cell Efficiency, June 1, 2011, <https://eere-exchange>.

- energy.gov/Default.aspx#1767d3fc-9c9e-4c93-bb3e-6d93cecf0105f .
12. Swanson RM. The Promise of Concentrators. *Progress in Photovoltaics: Research and Applications* 2000; **8**: 93–111.
 13. Green MA. Third generation photovoltaics: ultra-high conversion efficiency at low cost. *Progress in Photovoltaics: Research and Applications* 2001; **9**: 123, doi: 10.1002/pip.360.
 14. Ermer JH, Jones RK, Hebert P, Pien P, King RR, Bhusari D, Brandt R, Al-Taher O, Fetzer C, Kinsey GS, Karam N. Status of C3MJ+ and C4MJ Production Concentrator Solar Cells at Spectrolab. *37th IEEE Photovoltaic Specialists Conf. (PVSC), Seattle, Washington* 2011.
 15. King RR, Law DC, Edmondson KM, Fetzer CM, Kinsey GS, Yoon H, Sherif RA, Krut DD, Ermer JH, Hebert P, Pien P, Karam NH. Multijunction Solar Cells with Over 40% Efficiency and Future Directions in Concentrator PV. *22nd European Photovoltaic Solar Energy Conf., Milan, Italy* 2007; 11–15.
 16. King RR, Bhusari D, Boca A, Larrabee D, Liu X-Q, Hong W, Fetzer CM, Law DC, Karam NH. Band gap-voltage offset and energy production in next-generation multijunction solar cells. *Progress in Photovoltaics: Research and Applications* 2011; **19**: 797–812, doi: 10.1002/pip.1044, and *5th World Conf. on Photovoltaic Energy Conversion and 25th European Photovoltaic Solar Energy Conf., Valencia, Spain, Sep. 2010*, pp. 33–46.
 17. King RR, Haddad M, Isshiki T, Colter P, Ermer J, Yoon H, Joslin DE, Karam NH. Metamorphic GaInP/GaInAs/Ge Solar Cells. *28th IEEE Photovoltaic Specialists Conf. (PVSC), Anchorage, Alaska* 2000; 982–985.
 18. King RR, Sherif RA, Law DC, Yen JT, Haddad M, Fetzer CM, Edmondson KM, Kinsey GS, Yoon H, Joshi M, Mesropian S, Cotal HL, Krut DD, Ermer JH, Karam NH. New Horizons in III-V Multijunction Terrestrial Concentrator Cell Research. *21st European Photovoltaic Solar Energy Conf., Dresden, Germany* 2006; 124–128.
 19. U.S. Pat. No. 6,316,715, Multijunction Photovoltaic Cell with Thin 1st (Top) Subcell and Thick 2nd Subcell of Same or Similar Semiconductor Material. R. R. King, D. E. Joslin, N. H. Karam, filed Mar. 15, 2000, issued Nov. 13, 2001.
 20. Geisz JF, Friedman DJ, Olson JM, Kurtz SR, Keyes BM, *Journal of Crystal Growth* 1998; **195**: 401.
 21. Kurtz SR, Allerman AA, Seager CH, Sieg RM, Jones ED, *Applied Physics Letters* 2000; **77**: 400.
 22. Kurtz SR, Allerman AA, Jones ED, Gee JM, Banas JJ, Hammons BE, *Applied Physics Letters* 1999; **74**: 729.
 23. Li JZ, Lin JY, Jiang HX, Geisz JF, Kurtz SR, *Applied Physics Letters* 1999; **75**: 1899.
 24. Kurtz S, Geisz JF, Friedman DJ, Metzger WK, King RR, Karam NH, *Journal of Applied Physics* 2004; **95**: 2505.
 25. Kurtz S, Geisz JF, Keyes BM, Metzger WK, Friedman DJ, Olson JM, Ptak AJ, King RR, Karam NH, *Applied Physics Letters* 2003; **82**: 2634.
 26. Volz K, Torunski T, Lackner D, Rubel O, Stolz W, Baur C, Muller S, Dimroth F, Bett AW. Material development for improved 1 eV (GaIn)(NAs) solar cell structures. *Transaction of the ASME* 2007; **129**: 266.
 27. Volz K, Lackner D, Nemeth I, Kunert B, Stolz W, Baur C, Dimroth F, Bett AW. Optimization of annealing conditions of (GaIn)(NAs) for solar cell applications. *Journal of Crystal Growth* 2008; **310**: 2222.
 28. Jackrel DB, Bank SR, Yuen HB, Wistey MA, Harris JS, Jr., Ptak AJ, Johnston SW, Friedman DJ, Kurtz SR, *Journal of Applied Physics* 2007; **101**: 114916.
 29. King RR, Fetzer CM, Edmondson KM, Law DC, Colter PC, Cotal HL, Sherif RA, Yoon H, Isshiki T, Krut DD, Kinsey GS, Ermer JH, Kurtz S, Moriarty T, Kiehl J, Emery K, Metzger WK, Ahrenkiel RK, Karam NH. Metamorphic III-V Materials, Sublattice Disorder, and Multijunction Solar Cell Approaches with Over 37% Efficiency. *Proc. 19th European Photovoltaic Solar Energy Conf., Paris, France, June 7–11, 2004*; 3587–3593.
 30. King RR, Law DC, Fetzer CM, Sherif RA, Edmondson KM, Kurtz S, Kinsey GS, Cotal HL, Krut DD, Ermer JH, Karam NH. Pathways to 40%-Efficient Concentrator Photovoltaics. *Proc. 20th European Photovoltaic Solar Energy Conf., Barcelona, Spain, June 6–10, 2005*; 118–123.
 31. King RR, Boca A, Hong W, Liu X-Q, Bhusari D, Larrabee D, Edmondson KM, Law DC, Fetzer CM, Mesropian S, Karam NH. Band-Gap-Engineered Architectures for High-Efficiency Multijunction Concentrator Solar Cells. *24th European Photovoltaic Solar Energy Conf., Hamburg, Germany, Sep. 21–25, 2009*; 55–61.
 32. Létay G, Baur C, Bett AW. Theoretical Investigations of III-V Multi-junction Concentrator Cells Under Realistic Spectral Conditions. *19th European Photovoltaic Solar Energy Conf.* 2004; 187–190.
 33. King RR, Sherif RA, Law DC, Yen JT, Haddad M, Fetzer CM, Edmondson KM, Kinsey GS, Yoon H, Joshi M, Mesropian S, Cotal HL, Krut DD, Ermer JH, Karam NH. New Horizons in III-V Multijunction Terrestrial Concentrator Cell Research. *21st European Photovoltaic Solar Energy Conference (EU PVSEC), Dresden, Germany* 2006; 124, ISBN 3-936338-20-5.

34. Kinsey GS, Edmondson KM. Spectral response and energy output of concentrator multijunction solar cells. *Progress in Photovoltaics: Research and Applications* 2009; **17**: 279–288, doi: 10.1002/pip.
35. Newman F, Aiken D, Patel P, Chumney D, Aeby I, Hoffman R, Sharps P. Optimization of inverted metamorphic multijunction solar cells for field-deployed concentrating PV systems. *34th IEEE Photovoltaic Specialists Conference (PVSC) 2009*; 1611–1616, doi: 10.1109/PVSC.2009.5411385
36. Philipps SP, Peharz G, Hoheisel R, Hornung T, Al-Abbadi NM, Dimroth F, Bett AW. Energy harvesting efficiency of III-V triple-junction concentrator solar cells under realistic spectral conditions. *Solar Energy Materials and Solar Cells* 2010; **94**: 869–877, ISSN 0927–0248, doi: 10.1016/j.solmat.2010.01.010.
37. Dimroth F, Philipps SP, Peharz G, Welsch E, Kellenbenz R, Roesener T, Klinger V, Oliva E, Steiner M, Meusel M, Guter W, Bett AW. Promises of Advanced Multijunction Solar Cells for the Use in CPV Systems. *35th IEEE Photovoltaic Specialists Conf. (PVSC), Honolulu, HI* 2010.
38. Spectrolab data sheet, CPV Point Focus Solar Cells, C4MJ Metamorphic Fourth Generation CPV Technology, July 12, 2011, http://www.spectrolab.com/Data-Sheets/PV/CPV/C4MJ_40Percent_Solar_Cell.pdf.
39. Verlinden PJ, Lewandowski A, Bingham C, Kinsey GS, Sherif RA, Lasich JB. Performance and Reliability of Multijunction III-V Modules for Concentrator Dish and Central Receiver Applications. *4th World Conf. on Photovoltaic Energy Conversion (WCPEC), Waikoloa, Hawaii* 2006.

APPENDIX A

The economic benefits of high-efficiency are straightforward to calculate. In a simplified approach, the system cost per unit of generated energy, $(C/E)_{\text{system}}$, is the cost of the system per unit module aperture area, divided by the energy per area generated over a given payback time:

$$\begin{aligned} \left(\frac{C}{E}\right)_{\text{system}} &= \frac{\frac{C_{\text{mod}}}{A_{\text{mod}}} + \frac{C_{\text{tracking}}}{A_{\text{mod}}} + \frac{C_{\text{BOS, area}}}{A_{\text{mod}}} + \frac{C_{\text{IMF}}}{A_{\text{mod}}} + \frac{C_{\text{pwr cond}}}{A_{\text{mod}}}}{Int_{\text{annual avg}} \eta_{\text{AC, system}} T_{\text{payback}}} \\ &= \frac{(C_{\text{cell}} + C_{\text{cell pkg}}) \left(\frac{1}{R_{\text{geo}}}\right) + \frac{C_{\text{mod pkg}}}{A_{\text{mod}}} + \frac{C_{\text{tracking}}}{A_{\text{mod}}} + \frac{C_{\text{BOS, area}}}{A_{\text{mod}}} + \frac{C_{\text{IMF}}}{A_{\text{mod}}} + \left(\frac{C_{\text{pwr cond}}}{P_{\text{system, rated}}}\right) Int_{\text{inc, rated}} \eta_{\text{AC, system}}}{Int_{\text{annual avg}} \eta_{\text{AC, system}} T_{\text{payback}}} \end{aligned} \quad (\text{A1})$$

in units of \$/kWh of generated electricity, where:

$$\frac{C_{\text{mod}}}{A_{\text{mod}}} = \frac{(C_{\text{cell}} + C_{\text{cell pkg}})}{A_{\text{cell}}} \left(\frac{1}{R_{\text{geo}}}\right) + \frac{C_{\text{mod pkg}}}{A_{\text{mod}}} \quad (\text{A2})$$

$$P_{\text{system, rated}} = Int_{\text{inc, rated}} \eta_{\text{AC, system}} A_{\text{mod}} \quad (\text{A3})$$

and:

$C_{\text{cell}} =$	cost of solar cells in system
$C_{\text{cell pkg}} =$	cost of cell packaging (excl. cell), e.g., ceramic mount, electrical interconnects, bypass diode, secondary concentrator, other elements of receiver package
$C_{\text{mod pkg}} =$	cost of module packaging (excl. cells and cell packaging), e.g., glazing, lenses or mirrors of primary concentrator, encapsulation, module housing, etc.
$C_{\text{tracking}} =$	cost of tracking mechanism
$C_{\text{BOS, area}} =$	cost of area-related balance-of-system (BOS) hardware (excl. tracking and power conditioning), e.g., support structures, wiring
$C_{\text{IMF}} =$	cost of installation, operations and maintenance, and financing
$C_{\text{pwr cond}} / P_{\text{system, rated}} =$	cost of power conditioning unit (inverter) for system, divided by rated power output of system
$A_{\text{cell}} =$	aperture area of cells in system
$A_{\text{mod}} =$	aperture area of modules in system
$R_{\text{geo}} =$	geometric concentration ratio of system $\equiv A_{\text{mod}} / A_{\text{cell}}$
$Int_{\text{inc, rated}} =$	incident intensity of sunlight at which system power is rated, typically 1000 W/m ²
$Int_{\text{annual avg}} =$	intensity of solar resource (direct normal for concentrator system, global for flat-plate system) in a given geographic location, typically in units of kWh/(m ² day)
$T_{\text{payback}} =$	time allotted to pay back capital cost of system, using revenue from power generated
$\eta_{\text{AC, system}} =$	total efficiency of PV system, from sunlight to AC power.

Equation A1 is the same as Eqn. 1 discussed earlier, but with greater detail in the costs shown, because C_{BOS} in Eqn

$$\left(\frac{C}{P}\right)_{\text{system}} = \frac{C_{\text{mod}} + C_{\text{tracking}} + C_{\text{BOS, area}} + C_{\text{IMF}} + C_{\text{pwr cond}}}{P_{\text{system, rated}}}$$

$$= \frac{\frac{C_{\text{mod}}}{A_{\text{mod}}} + \frac{C_{\text{tracking}}}{A_{\text{mod}}} + \frac{C_{\text{BOS, area}}}{A_{\text{mod}}} + \frac{C_{\text{IMF}}}{A_{\text{mod}}} + \frac{C_{\text{pwr cond}}}{A_{\text{mod}}}}{Int_{\text{inc, rated}} \eta_{\text{AC, system}}}$$

such that: (A4)

$$\left(\frac{C}{P}\right)_{\text{system}} = \left(\frac{C}{E}\right)_{\text{system}} \left(\frac{Int_{\text{annual avg}} T_{\text{payback}}}{Int_{\text{inc, rated}}}\right) \quad (A5)$$

in units of \$/W.

For the four cases discussed in the text, the cost parameters consistent with the US Department of Energy current ‘‘Business as Usual’’ 2016 cost projections for utility scale PV systems [11] that were used in this study are tabulated below in Table II. These costs do not explicitly

include land costs, because the cost of land is highly variable depending on specific location. Land costs may be folded into $C_{\text{BOS, area}}$ if desired, because it is an area-related cost. The cost of land for photovoltaic systems is often smaller than one might expect, especially for remote desert areas used for some utility-scale PV fields, or essentially free on flat commercial rooftops or buildings already owned by the PV customer. Additional costs associated with tracking mechanisms for concentrator photovoltaic systems are included and are also tabulated below in Table II.

APPENDIX B

The total system efficiency is the product of $\eta_{\text{cell, STC}}$, the solar cell efficiency at standard test conditions (STC), and several other efficiencies

$$\eta_{\text{AC, system}} = \eta_{\text{cell, STC}} \eta_{\text{optical}} \eta_{\text{pwr cond}} f_{\text{temp}} f_{\text{current mismatch, design vs. avg. spectrum}} f_{\text{current mismatch, changing spectrum}} f_{\text{tracking error}} \quad (B1)$$

Table II. Economic and performance input parameters, and the calculated cost-effectiveness threshold for $Int_{\text{annual avg}}$ in units of (kWh/(m² day)), shown in bold, for the four CPV system cases discussed in the paper.

CPV system costs		Case 1	Case 2	Case 3	Case 4
Cell technology		III-V MJ	III-V MJ	III-V MJ	Silicon CPV
Cell eff. at STC		40%	50%	50%	26%
Optical efficiency of CPV system		80%	80%	85%	80%
Intensity on cell (W/cm ²)		50.0	50.0	85.0	50.0
Given $(C/E)_{\text{system}} = 0.14$ \$/kWh, threshold for cost effectiveness occurs at					
$Int_{\text{annual avg}}$ (kWh/(m ² day))		5.84	4.76	4.10	7.46
$C_{\text{pwr cond}}/P_{\text{system, rated}}$ (\$/W)		0.18	0.18	0.18	0.18
$(C_{\text{BOS}} + C_{\text{IMF}})/P_{\text{system, rated}}$ (\$/W)		0.97	0.78	0.73	1.58
$C_{\text{tracking}}/P_{\text{system, rated}}$ (\$/W)		0.19	0.15	0.14	0.31
$C_{\text{mod}}/P_{\text{system, rated}}$ (\$/W)		1.05	0.84	0.62	0.98
$C_{\text{system}}/P_{\text{system, rated}}$ (\$/W)		2.39	1.95	1.68	3.05
$C_{\text{cell}}/A_{\text{cell}}$ (\$/cm ²)		7.50	7.50	7.50	0.00
$C_{\text{cell pkg}}/A_{\text{cell}}$ (\$/cm ²)		2.50	2.50	2.50	2.50
$\eta_{\text{cell, STC}}$ (%)		40%	50%	50%	26%
R_{geo} (unit less)		625	625	1000	625
η_{optical} (%)		80%	80%	85%	80%
Intensity on cell (W/cm ²)		50.0	50.0	85.0	50.0
$\eta_{\text{AC, system}}$ (%)		26.8%	33.5%	35.6%	16.5%
$Int_{\text{inc, rated}}$ (W/m ²)		1000	1000	1000	1000
T_{payback} (years)		8	8	8	8
$C_{\text{cell}}/A_{\text{mod}}$ (\$/m ²)		120	120	75	0
$C_{\text{cell pkg}}/A_{\text{mod}}$ (\$/m ²)		40	40	25	40
$C_{\text{mod}}/A_{\text{mod}}$ (\$/m ²)		122	122	122	122
$C_{\text{pwr cond}}/A_{\text{mod}}$ (\$/m ²)		48	60	64	30
$(C_{\text{BOS}} + C_{\text{IMF}})/A_{\text{mod}}$ (\$/m ²)		260	260	260	260
$C_{\text{tracking}}/A_{\text{mod}}$ (\$/m ²)		51	51	51	51
$C_{\text{mod}}/A_{\text{mod}}$ (\$/m ²)		282	282	222	162
$C_{\text{system}}/A_{\text{mod}}$ (\$/m ²)		642	654	597	503

STC, standard test conditions; CPV, concentrator photovoltaic or concentrator photovoltaics.

Table III. Efficiency and performance factors contributing to overall CPV system efficiency, shown in bold, for the four CPV system cases described in the text.

CPV system efficiency												
Cell technology	Cell eff. at (STC)	Optical efficiency of CPV system	Intensity on cell (W/cm ²)	$\eta_{AC, system}$	$\eta_{cell, STC}$	$\eta_{pwr cond}$	f_{temp}	$f_{current mismatch, design vs. avg. spectrum}$		$f_{current mismatch, changing spectrum}$	$f_{tracking error}$	
				$\eta_{AC, system}$	$\eta_{cell, STC}$							
Case 1	III-V MJ	40%	80%	50.0	26.8%	40%	80%	97%	0.925	0.99	0.954	0.99
Case 2	III-V MJ	50%	80%	50.0	33.5%	50%	80%	98%	0.925	0.99	0.944	0.99
Case 3	III-V MJ	50%	85%	85.0	35.6%	50%	85%	98%	0.925	0.99	0.944	0.99
Case 4	Silicon CPV	26%	80%	50.0	16.5%	26%	80%	97%	0.825	1.0	1.0	0.99

STC, standard test conditions; CPV, concentrator photovoltaic or concentrator photovoltaics.

where:

$\eta_{optical} =$	efficiency of system optics (e.g., primary and secondary concentrators)
$\eta_{pwr cond} =$	efficiency of power conditioning unit
$f_{temp} =$	fraction of power at STC remaining at operating temperature
$f_{current mismatch, design vs. avg. spectrum} =$	fraction of power remaining because of the difference between the standard design solar spectrum and average actual spectrum
$f_{current mismatch, changing spectrum} =$	fraction of energy production remaining because of changes in the actual spectrum over the day and year, with respect to the average actual spectrum
$f_{tracking error} =$	fraction of energy production remaining because of tracking errors

For the four cases discussed in the text, the various contributions to concentrator photovoltaic (CPV) system efficiency that were used in this study are tabulated below in Table III:

For the temperature dependence, a temperature delta of 50 °C was assumed between an operating temperature of 75 °C and the temperature at STC of 25 °C. The power temperature coefficient used was -0.15 relative%/°C for III-V multijunction cells (-0.06 absolute%/°C in efficiency) [4], and -0.35 relative%/°C for high-efficiency silicon back contact CPV cells [5]. In practical applications, the spectrum for which the subcells in a multijunction cell are designed to be current matched, the design spectrum, may be somewhat different than the average spectrum under actual operating conditions, as discussed in [14]. This can reduce the energy production of the multijunction cell and is accounted for in Eqn B1 with the factor $f_{current mismatch, design vs. avg. spectrum}$. Additionally, the actual spectrum at any given time is typically different than the average actual spectrum, contributing to current mismatch among subcells, and reducing the overall energy production of the multijunction cell. This effect is quantified by the factor $f_{current mismatch, changing spectrum}$ in Eqn B1 and was modeled as the spectrum utilization factor over day in [16], as shown in Table I. The modeled values for this spectrum utilization factor of 0.954 for a 3-junction cell were used in Case 1 for a 40% efficient cell, and 0.944 for a 5-junction cell was used for Cases 2 and 3 for 50% efficient cells, as shown in Table III.